Available online at www.sciencedirect.com

ScienceDirect

Energy Procedia 137 (2017) 26–37

Energy Procedia

www.elsevier.com/locate/procedia

14th Deep Sea Offshore Wind R&D Conference, EERA DeepWind'2017, 18-20 January 2017, Trondheim, Norway

Can a Wind Turbine Learn to Operate Itself? Evaluation of the potential of a heuristic, data-driven self-optimizing control system for a 5MW offshore wind turbine

Stefan Gueorguiev Iordanov[a], Maurizio Collu[a,*], Yi Cao[a]

[a]*Cranfield University, Cranfield, Bedfordshire MK43 0AL, United Kingdom*

Abstract

Larger and more expensive offshore wind turbines, subject to more complex loads, operating in larger wind farms, could substantially benefit from more advanced control strategies. Nonetheless, the wind industry is reluctant to adopt such advanced, more efficient solutions, since this is perceived linked to a lower reliability. Here, a relatively simple self-optimizing control strategy, capable to "learn" (data-driven) which is the optimum control strategy depending on the objective defined, is presented. It is proved that it "re-discovers", model-free, the optimum strategy adopted by commercial wind turbine in region 2. This methodology has the potential to achieve advanced control performance without compromising its simplicity and reliability.

Peer-review under responsibility of SINTEF Energi AS.

Keywords: wind turbines; advanced control systems; data-driven; self-optimising control

1. Introduction

Due to the high costs of offshore wind turbines, their reliability is a key parameter, driving the cost of the energy delivered to the grid. Consequently, the wind industry is, in general, reluctant to adopt more advanced control strategies, and relies on simpler control structures: it is difficult to develop a control algorithm delivering both efficiency and reliability, since in general the two aspects involve conflicting objectives [1].

* Corresponding author. Tel.: +44 (0)1234 75 4779
E-mail address: maurizio.collu@cranfield.ac.uk

1876-6102
Peer-review under responsibility of SINTEF Energi AS.
10.1016/j.egypro.2017.10.332

On the other hand, larger and more expensive wind turbines (WT), subject to more complex aero-hydro-servo-elastic dynamics, operating in larger wind farms (more complex turbine-to-turbine interactions), could substantially benefit from more advanced control strategies [1]. Another important aspect is that modern WTs, through their monitoring systems, have already access to a large amount of sensor signals – but the large majority is not used for controlling the wind turbine, only to monitor the operational status for maintenance purposes. This is because the simpler control strategies adopted cannot handle a large number of sensor signals without compromising their simplicity and/or reliability, missing an opportunity to improve the wind turbine performance.

The ideal control system would be able to consider a large number of measurements, to optimally control the wind turbine, without escalating its complexity and therefore compromising its reliability, to be ease of use, and having low maintenance costs. This is the aim of the data-driven self-optimizing control strategy proposed.

1.1. Brief overview of advanced control systems for wind turbines

Some advanced control approaches, used to maximize the power output between the cut-in and the rated wind speed (region 2), rely on the wind speed as input. Johnson [2] proposes an adaptive controller which uses a simple gain adaptation law, designed to track the optimal gain. However, using wind speed as a direct input is technically challenging, e.g. it is difficult to obtain a representative wind speed measurement, and the performance of the control system is closely related to the quality of the sensor signal [3]. Thus, various approaches representing the wind speed not as a sensor signal but as a disturbance have been developed, as the Takagi–Sugeno–Kang model [5], where an adaptive fuzzy controller is proposed, which can continuously optimize its internal parameters to achieve optimal operation. Iyasere [6] presents a nonlinear controller, with blade pitch and tip speed ratio regulation optimized to track the maximum power coefficient operating point. Despite all the advantages, they are seldom used in industry, as they are perceived as too complex and costly to implement and to maintain. A comprehensive review of advanced control systems for wind turbines is presented in [1].

Nomenclature

AHSE	Aero-Hydro-Servo-Elastic (coupled model of dynamics)
WT	Wind Turbine
C_P	Coefficient of Power
CV	Controlled Variable
NREL	National Renewable Energy Laboratory (USA)
gSOC	generalised Self-Optimising Control
TSR	Tip Speed Ratio
NCO	Necessary Conditions for Optimality
P	Power (generator)

2. Generalised Self-Optimising Control: theory and application to wind turbines

Self-optimizing control (SOC) consists of defining functions of the process variables such that, when held constant, optimal operation is achieved, despite varying disturbances [4]. These controlled variables (CVs) are selected such that the system operates minimizing the loss of optimality with respect to a given cost function, generally related to the system economic performance [7]. By considering the effect of the transient response to the disturbance on the cost (objective) function negligible [5], the objective function J depends on the value of the manipulated variables (u), measurements (y), and disturbances (d) as in Eq. (1).

$$J = \varphi(u, y, d) \tag{1}$$

To select the CVs, a dynamics model of the system is developed and used off-line, to examine the structure of the optimal solution. However, a model based approach, often nonlinear, inevitably requires the linearization around the nominal operating points, resulting in potentially large inaccuracies due to linearization errors. To address this issue, Cao proposed a model-free approach [6]. This global SOC (gSOC) method relies entirely on the operational data representing the entire operating space to determine, in a single regression step, the CVs approximating the unmeasured necessary conditions of optimality (NCO), with zero set point to achieve near optimal operation globally [7]. Then, the deviation of the objective function in a reference point with respect to a neighborhood point can be approximated as in Eq. (2).

$$J_{i+1} - J_i = \sum_{j=1}^{n_u} \frac{dJ}{du_j}(u_{i+1,j} - u_{i,j}) \tag{2}$$

where n_u is the number of manipulated variables. The CVs can be linear or nonlinear measurement functions in the form of $CV = CV(y, \theta)$, θ to be obtained through regression such that (Eq. (3)):

$$CV(y, \theta) = \frac{dJ}{du} = 0 \tag{3}$$

Consequently, for a set of data u_i, y_i and J_i with d_i unknown, θ is obtained such that

$$min_\theta \sum_{i=1}^{N} \sum_{p=i_1}^{i_k} (J_p - J_i - \sum_{j=1}^{n_u} CV_j(y, \theta)(u_{p,j} - u_{i,j}))^2 \qquad i = 1, \dots, N \tag{4}$$

where $i_1, \dots, i_k$ are k neighborhood points i.

In the present case study, a gSOC approach is applied to derive the optimal control law for a 5MW offshore wind turbine[8]. Thanks to the prior learning of the structure of the optimal solution, the data-driven gSOC allows the system to regulate independently both pitch (β) and torque (Γ) to achieve near optimal operation globally. For the present case study, the manipulated variables u measurements y, and disturbance d are defined as:

$$u = [\Gamma, \beta], \quad y = [\Gamma, \beta, \omega_G, P], \quad d = [v] \tag{5}$$

Where ω_G is the generator rotational speed, P is the generator power, and v corresponds to wind speed velocity. If η is the generator efficiency, the objective function to be maximized is the electrical power output P:

$$P = \Gamma \cdot \omega_G \cdot \eta \tag{6}$$

The deviation of power in a reference point with respect to a neighborhood point can be expressed as in Eq. (7).

$$P_{i+1} - P_i = \frac{dP}{d\Gamma}(\Gamma_{i+1} - \Gamma_i) + \frac{dP}{d\beta}(\beta_{i+1} - \beta_i) \tag{7}$$

Two different combinations of measurement functions have been considered for the CVs. Measurement function one is shown in Eq. (8) and (9), while the measurement function two is shown in Eq. (10) and (11).

$$CV_1 = \theta_0 + \theta_1 \cdot \omega_G + \theta_2 \cdot \Gamma \tag{8}$$

$$CV_2 = \theta_3 + \theta_4 \cdot \omega_G + \theta_5 \cdot \beta \tag{9}$$

$$CV_3 = \theta_0 + \theta_1 \cdot \omega_G + \theta_2 \cdot P + \theta_3 \cdot \Gamma \tag{10}$$

$$CV_4 = \theta_4 + \theta_5 \cdot \omega_G + \theta_6 \cdot P + \theta_7 \cdot \beta \tag{11}$$

The CVs can be chosen to approximate NCO over the whole operating region by using a regression method or other function fitting methods [7]. The general procedure consists on sampling the whole operation space using independently generated inputs and disturbances. Once the measurements are obtained for all samples, the system behavior is fitted using a linear/non-linear function, $\hat{x}_i = \varphi(y_i, \theta)$, deriving the parameter θ_i to minimize Eq. (4).

To achieve a control structure capable of maximizing power through the gSOC approach in region 2, and saturate at rated power in region 3, a cascade structure for self-optimizing and constrained control as proposed by Cao is used [5] (Fig. 1).

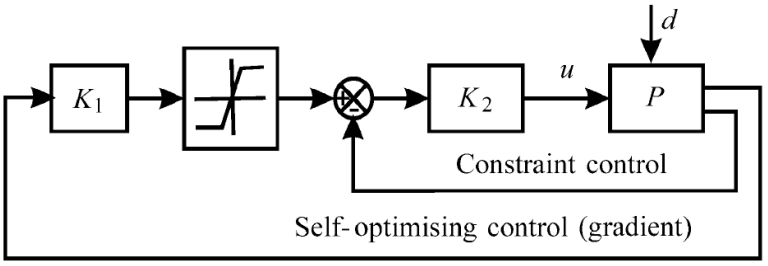

Fig. 1. Cascade structure for constrained self-optimizing control

The set point of the inner loop is given by a saturation block in the outer loop. This limits the set point within the constraints when disturbance cause the process move outside of the gSOC operating region. However, within the range of optimal operation, the set point of the inner loop is floating to perform a gSOC.

2.1. Conditional block for low speed operation

In control regions 1, 1 ½ and 2 ½, the turbine must be accelerated, then linearly brought to region 2 and then linearly brought again to region 3: a conditional block adjusts the gSOC input value, depending on the generator speed, adjusted as shown in Fig. 2

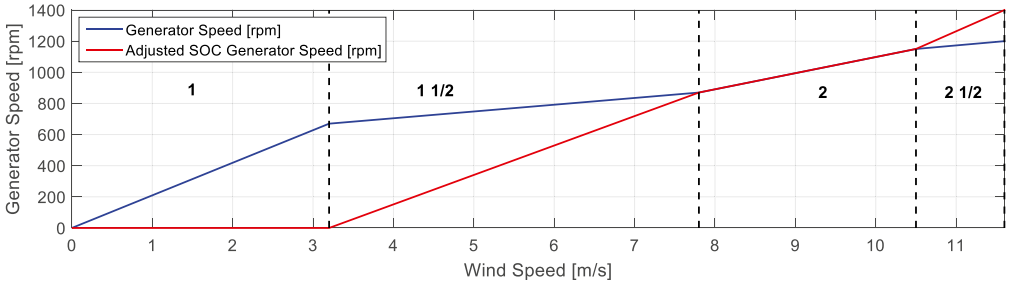

Fig. 2. Generator speed adjustment by the conditional block

- In region 1 (between 0 and 670 rpm), the input value for the gSOC control is 0: the power set point is then 0 as the generator torque.
- In region 1 ½ , the input generator speed of the gSOC control is linearly adjusted from 0 rpm when real generator speed is 660 rpm, to 870 rpm when real generator speed is 870 rpm.
- In region 2, the gSOC must keep the WT operation at maximum power output. During this region the gSOC input is the real generator speed.
- In region 2 ½ , the input generator speed of the gSOC control is linearly adjusted from 1150 rpm when real generator speed is 1150 rpm, to 1404 rpm when real generator speed is 1200 rpm. This last region is needed to bring the P in region 3 to the rated power at rated speed (5 MW and 1200 rpm), which is not an operating point corresponding to the optimal solution.

3. Methodology

The present methodology does not need a model of dynamics to be implemented (model-free approach), but due to the difficulty in collecting real-word operational data from multi-MW offshore wind turbine, a series of synthetic operational data have been generated, using a aero-hydro-servo-elastic coupled model of dynamics. A conventional control system (baseline control, BC) has been adopted, to be used as benchmark. The results from these simulations (§3.2) have been used to derive the coefficients of the controlled variables, in Eq. (8)(9)(10)(11).

Then, the derived CVs have been implemented as alternative control strategy for the 5MW WT, and the gSOC strategy has been tested using constant and turbulent wind fields. The gSOC performance is then compared against the BC performance.

3.1. AHSE model, reference wind turbine, and baseline control system

FAST v8 has been used , since it includes an interface to couple it with Simulink®, allowing the user to develop advanced WT control systems [9]. As representative offshore wind turbine system, the well-known NREL 5MW offshore reference WT has been chosen [8]. As a benchmark control approach, the baseline control (BC) system developed in [8] has been implemented in Simulink.

3.2. Simulations to generate the operational data

The necessary simulations have been carried out by fixing the value of the disturbance (wind speed). For each disturbance value, 120 samples are taken: 20 samples are taken at a constant blade pitch angle, between -3° and 2°, plus a random value between 0 and 1. In order to obtain sampling data near the optimum operating point, and also to avoid applying higher generator torque than the aerodynamic torque, the initial torque for each 20 sample group is fixed using Eq. (12), which depends on the disturbance value. Then, torque is increased in each sample following Eq. (13). It must be noticed that Eq. (12) is not strictly necessary, and it has been adopted only to speed up the procedure (otherwise FAST would have crashed or the transient would have taken longer).

$$\Gamma_1 = -3193.9 + 167.5 \times wind + 307.4 \times wind^2 + u([0,10]) \tag{12}$$

$$\Gamma_{i+1} = \Gamma_i + 100 + u([0,80]) + u([0,120]), \quad i = 1, \ldots, 20 \tag{13}$$

$$[-3° + R \quad -2° + R \quad -1° + R \quad 0° + R \quad 1° + R \quad 2° + R], \qquad R \sim U([0,1])$$

$$\begin{bmatrix} \Gamma_1 \\ \Gamma_2 \\ \vdots \\ \Gamma_{19} \\ \Gamma_{20} \end{bmatrix} \Rightarrow \begin{bmatrix} X_{1,1} & X_{1,2} & X_{1,3} & X_{1,4} & X_{1,5} & X_{1,6} \\ X_{2,1} & X_{2,2} & X_{2,3} & X_{2,4} & X_{2,5} & X_{2,6} \\ \vdots & \vdots & \vdots & \vdots & \vdots & \vdots \\ X_{19,1} & X_{19,2} & X_{19,3} & X_{19,4} & X_{19,5} & X_{19,6} \\ X_{20,1} & X_{20,2} & X_{20,3} & X_{20,4} & X_{20,5} & X_{20,6} \end{bmatrix}$$

Fig. 3. Structure of the sample matrix for every disturbance value

The torque and pitch increase from a reference sample to a neighbor have been randomized, to avoid that the regression coefficients get biased by constant increases in blade pitch or generator torque. Fig. 3 illustrates the structure of the data collection. Each disturbance step is composed of 5 matrices of 120 samples corresponding to: generator power output, generator speed, generator torque, blade pitch, wind speed. 3720 samples are therefore obtained, from 6 to 12 m/s (constant increase 0.2 m/s), corresponding to 31 disturbance steps.

3.2.1. Regression to obtain the CVs coefficients

Eq. (7) is the expression used to carry out the least-square regression and determine the CVs, and is only valid for those neighboring operating points corresponding to the same disturbance value. By defining the CVs as:

$$\frac{dP}{d\Gamma} = CV_1 = \theta_0 + \theta_1 \cdot \omega_G + \theta_2 \cdot \Gamma \tag{14}$$

$$\frac{dP}{d\beta} = CV_2 = \theta_3 + \theta_4 \cdot \omega_G + \theta_5 \cdot \beta \tag{15}$$

Eq. (7) can be expressed as

$$P_{i+1} - P_i = (\theta_0 + \theta_1 \cdot \omega_G + \theta_2 \cdot \Gamma_i) \cdot (\Gamma_{i+1} - \Gamma_i) + (\theta_3 + \theta_4 \cdot \omega_G + \theta_5 \cdot \beta_i) \cdot (\beta_{i+1} - \beta_i) \tag{16}$$

Considering a sample matrix (17) corresponding to the same disturbance value,

$$[X_{i,j}], \qquad i = 1, \dots, 20, \qquad j = 1, \dots, 6 \tag{17}$$

the torque and pitch increase of a reference point with respect to a strict neighbor can be expressed as

$$\begin{bmatrix} \Delta\Gamma_{i+1,j} \\ \Delta\Gamma_{i,j+1} \\ \Delta\Gamma_{i+1,j+1} \end{bmatrix} = \begin{bmatrix} (\Gamma_{i+1,j} - \Gamma_{i,j}) \\ (\Gamma_{i,j+1} - \Gamma_{i,j}) \\ (\Gamma_{i+1,j+1} - \Gamma_{i,j}) \end{bmatrix}, \quad \begin{bmatrix} \Delta\beta_{i+1,j} \\ \Delta\beta_{i,j+1} \\ \Delta\beta_{i+1,j+1} \end{bmatrix} = \begin{bmatrix} (\beta_{i+1,j} - \beta_{i,j}) \\ (\beta_{i,j+1} - \beta_{i,j}) \\ (\beta_{i+1,j+1} - \beta_{i,j}) \end{bmatrix} \tag{18}$$

Fig. 4 illustrates the concept of strict neighbor. Data samples for regression are obtained from the submatrix 19x5, as the elements of the last column and last row do not have the three necessary neighbor points.

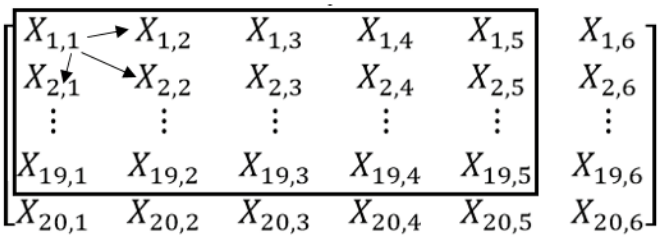

Fig. 4. Matrix element that have three strict neighbours

For each element of the submatrix indicated above, three data samples for the regression are obtained, as in Eq. (19); therefore from each sample matrix 285 samples are obtained. The method of least squares is a standard regression approach where the overall solution minimizes the error sum of squares(S_E). The partial input matrix X_k corresponding to a sample matrix obtained at a constant disturbance value is defined as the vertical concatenation of the 285 previously stated elements, as in Eq. (20).

$$\begin{bmatrix} P_{i+1,j} - P_{i,j} \\ P_{i,j+1} - P_{i,j} \\ P_{i+1,j+1} - P_{i,j} \end{bmatrix} \tag{19}$$

$$= \begin{bmatrix} \Delta\Gamma_{i+1,j} & \omega_{i,j} \cdot \Delta\Gamma_{i+1,j} & \Gamma_{i,j} \cdot \Delta\Gamma_{i+1,j} & \Delta\beta_{i+1,j} & \Delta\beta_{i+1,j} \cdot \omega_{i,j} & \Delta\beta_{i+1,j} \cdot \beta_{i,j} \\ \Delta\Gamma_{i,j+1} & \omega_{i,j} \cdot \Delta\Gamma_{i,j+1} & \Gamma_{i,j} \cdot \Delta\Gamma_{i,j+1} & \Delta\beta_{i,j+1} & \Delta\beta_{i,j+1} \cdot \omega_{i,j} & \Delta\beta_{i,j+1} \cdot \beta_{i,j} \\ \Delta\Gamma_{i+1,j+1} & \omega_{i,j} \cdot \Delta\Gamma_{i+1,j+1} & \Gamma_{i,j} \cdot \Delta\Gamma_{i+1,j+1} & \Delta\beta_{i+1,j+1} & \Delta\beta_{i+1,j+1} \cdot \omega_{i,j} & \Delta\beta_{i+1,j+1} \cdot \beta_{i,j} \end{bmatrix} \cdot \begin{bmatrix} \theta_0 \\ \theta_1 \\ \theta_2 \\ \theta_3 \\ \theta_4 \\ \theta_5 \end{bmatrix}$$

$$X_{k,i,j} = \begin{bmatrix} \Delta\Gamma_{i+1,j} & \omega_{i,j} \cdot \Delta\Gamma_{i+1,j} & \Gamma_{i,j} \cdot \Delta\Gamma_{i+1,j} & \Delta\beta_{i+1,j} & \Delta\beta_{i+1,j} \cdot \omega_{i,j} & \Delta\beta_{i+1,j} \cdot \beta_{i,j} \\ \Delta\Gamma_{i,j+1} & \omega_{i,j} \cdot \Delta\Gamma_{i,j+1} & \Gamma_{i,j} \cdot \Delta\Gamma_{i,j+1} & \Delta\beta_{i,j+1} & \Delta\beta_{i,j+1} \cdot \omega_{i,j} & \Delta\beta_{i,j+1} \cdot \beta_{i,j} \\ \Delta\Gamma_{i+1,j+1} & \omega_{i,j} \cdot \Delta\Gamma_{i+1,j+1} & \Gamma_{i,j} \cdot \Delta\Gamma_{i+1,j+1} & \Delta\beta_{i+1,j+1} & \Delta\beta_{i+1,j+1} \cdot \omega_{i,j} & \Delta\beta_{i+1,j+1} \cdot \beta_{i,j} \end{bmatrix} \tag{20}$$

$$i = 1, \dots, 19, \quad j = 1, \dots, 5 \quad k = 1, \dots, 31$$

The total input matrix X is defined as the vertical concatenation of X_k corresponding to the 31 step disturbances.

$$X = \begin{bmatrix} X_1 \\ \vdots \\ X_{31} \end{bmatrix} \tag{21}$$

In the same way, the partial output vector Y_k corresponds to the vertical concatenation of the 285 elements corresponding to the same disturbance value, Eq. (22).

$$Y_{k,i,j} = \begin{bmatrix} P_{i+1,j} - P_{i,j} \\ P_{i,j+1} - P_{i,j} \\ P_{i+1,j+1} - P_{i,j} \end{bmatrix} \tag{22}$$

The total output vector Y is defined as the vertical concatenation of the 31 partial output vectors, Eq. (23)

$$Y = \begin{bmatrix} Y_1 \\ \vdots \\ Y_{31} \end{bmatrix} \tag{23}$$

The regression coefficients θ are obtained by applying the least-squares regression, Eq. (24)

$$\theta = (X^T \cdot X)^{-1} \cdot X^T \cdot Y \tag{24}$$

The effectiveness of the regression is evaluated by using the R^2 parameter given by

$$R^2 = \frac{S_T - S_E}{S_T}, \qquad S_E = \sum_{i=1}^{N} (x_i - \hat{x}_i)^2, \quad S_T = \sum_{i=1}^{N} (x_i - \bar{x}_i)^2 \tag{25}$$

where S_T stands for the total sum of squares.

3.3. Controlled variable coefficients derivation and gSOC numerical implementation

The resulting control structure for the gSOC is represented in Fig. 5, with two cascade loops controlling the generator torque and the blade pitch angle. Torque is regulated by implementing a PI control on generator power. At the first control section, speed measurement is given to the conditional block, which adjusts the value depending on the control region (1,1 ½, 2, 2 ½) (§2.1). This value is then read by the two gSOC blocks in Eq. (26) and (27).

$$\Gamma: \frac{dP}{d\Gamma} = 0 \tag{26}$$

$$P: \frac{dP}{d\Gamma} = 0 \tag{27}$$

The gSOC block (26) derives the torque corresponding to the maximum power output at current disturbance value. Then, this value is passed to the gSOC block (27), which derives the power set point for the inner loop. The saturation block fixes the maximum power set point at a nominal rate of 5MW. In region 2, the pitch is controlled by the gSOC block (28). The saturation block in the outer loop restricts the actuation of the PI control.

$$\beta: \frac{dP}{d\beta} = 0 \tag{28}$$

Above rated power (5MW), the PI action overrides the gSOC block (28) actuation and regulates the blade pitch to positive values in order to reduce WT aerodynamic efficiency and maintain at nominal speed (1200 rpm).

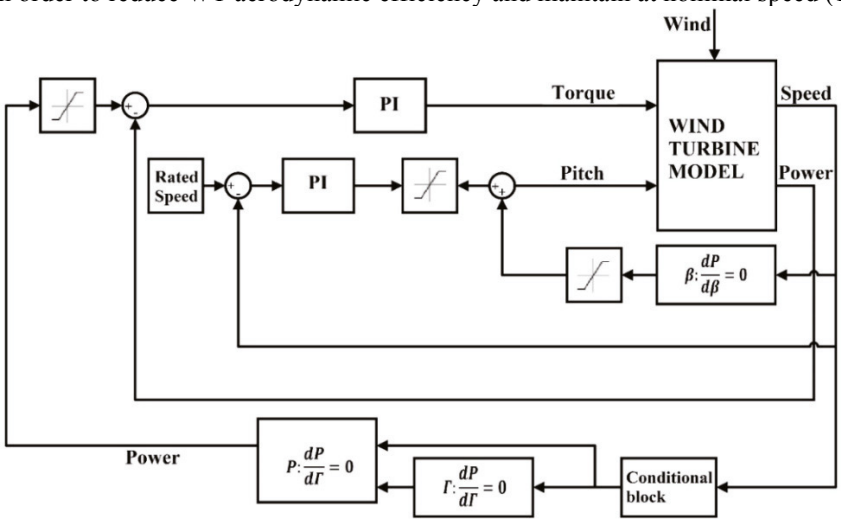

Fig. 5. Block diagram of the constrained self-optimizing control structure

4. Results

The two first control variables (Eq. (29) and (30)) are obtained as stated in §3.2, since the only measurements required are generator torque and rotational speed. The feedback control laws for Γ (Eq. (31)) and β (Eq. (32)) are obtained by setting the CVs to zero.

$$CV_1 = -0.198297281 + 0.000442821 \cdot \omega_G - 0.000007996 \cdot \Gamma \tag{29}$$

$$CV_2 = 38.151847922 - 0.122050002 \cdot \omega_G - 45.786177285 \cdot \beta \tag{30}$$

$$\Gamma = -24800 + 55.3803 \cdot \omega_G \tag{31}$$

$$\beta = 0.8333 - 0.0026 \cdot \omega_G \tag{32}$$

To perform a constrained gSOC, it is needed a third controlled variable used to determine the set point of the inner loop within the range of optimal operation. The input is the power regime corresponding to an optimal operation. Therefore, the second measurement functions must contain the generator power measurement (Eq. (33)).

$$CV_3 = 0.276306686 - 0.000209328 \cdot \omega_G + 0.000155259 \cdot P - 0.000018256 \cdot \Gamma \tag{33}$$

In region 2, the set point of the inner loop is given by Eq. (34).

$$P = -1779.65 + 1.3482 \cdot \omega_G + 0.1176 \cdot \Gamma \tag{34}$$

Table 1 shows the least-square error (R^2) for the regression corresponding to CV_1, CV_2 and CV_3.

Table 1. Least-square error for the CV resulting regressions

Controlled Variables	CV expression	R^2
CV_1, CV_2	(8), (9)	0.697
CV_3	(10), (11)	0.797

4.1. Results with steady wind speed

Fig. 6(a) and (b) show that the steady state action of the proposed constrained gSOC structure achieves the desired response for the whole WT operating region.

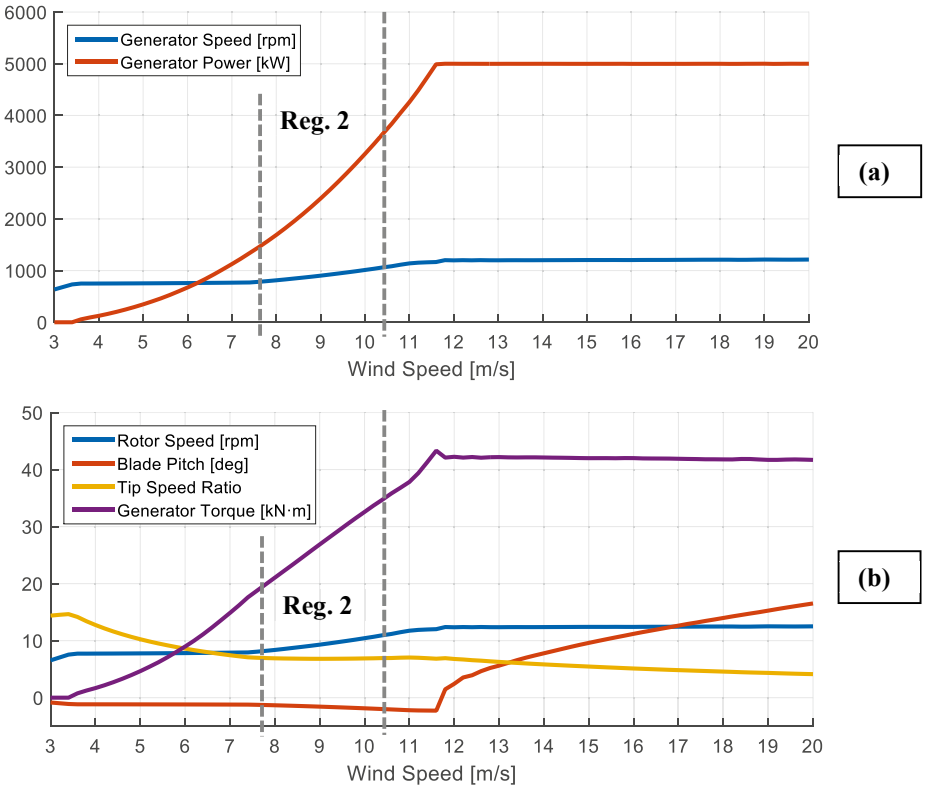

Fig. 6. Steady-state response vs wind speed, gSOC strategy

Fig. 7 shows the C_P versus TSR and blade pitch angle, for wind speeds from 6 to 12 m/s. The BC and gSOC trajectories are represented, and the marker size is proportional to the wind speed (steady-state operating point). The BC keeps blade pitch fixed at 0 deg, which constraints the max C_P to sub-optimal values. On the contrary, the gSOC makes use of both degrees of freedom to maximize C_P, as showed by the self-optimising control trajectory in Fig. 7, resulting in a higher energy capture.

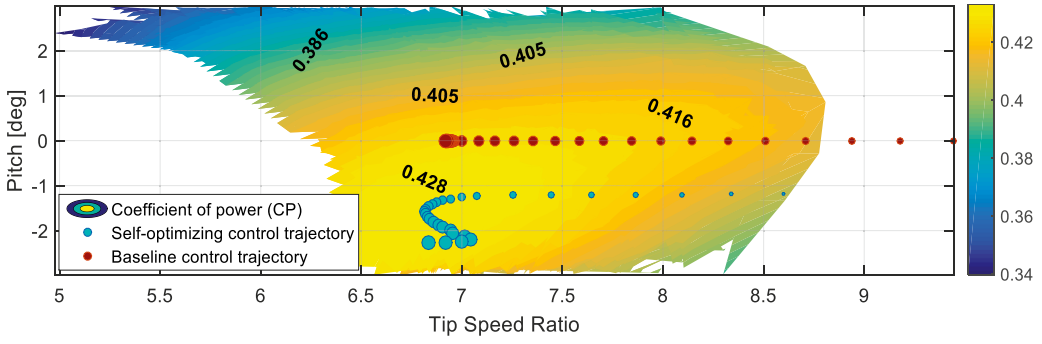

Fig. 7. Comparison between BC and gSOC trajectories for increasing wind ranged from 6 to 12 m/s

4.2. Results with turbulent wind speed

WT energy capture is evaluated for both gSOC and BC at different average speeds, within region 2. Total simulated time is 1300s, but the first 100s are not considered (transient). The energy generated is obtained by integrating the generator power output over time (Table 2).

Table 2. Comparison of self-optimizing control versus baseline control performance for turbulent wind regimes

Average wind speed [m/s] of the turbulent wind input file	Energy capture with gSOC [kJ]	Average power output for gSOC (kW)	Energy capture with BC [kJ]	Average power output for BC (kW)	Energy capture increase [%]	Average power output increase (kW)
7.5	1780513	1483.8	1771633	1476.4	0.50	7.4
8	2142346	1785.3	2128426	1773.7	0.65	11.6
8.5	2550473	2125.4	2535149	2112.6	0.60	12.8
9	2987486	2489.6	2974047	2478.4	0.45	11.2
9.5	3564322	2970.3	3549302	2957.8	0.42	12.5

5. Discussion

5.1. Can the wind turbine learn to (optimally) control itself?

Going back to the fundamental question posed by this paper, it can now be demonstrated that the wind turbine can indeed learn from experience how to operate itself with the gSOC strategy. The first proof is in Fig. 6(a). The gSOC objective function is the generator power P, and the gSOC strategy successfully maximizes P in region 2, without any knowledge of the dynamics of this relatively complex system, but only based on the operational data provided. The P curve is indeed very similar to the curve delivered by commercial multi-MW offshore wind turbines, and this is considered as the optimum strategy.

The second proof, more significant, is showed by analyzing how the gSOC strategy achieved this result (in Region 2). It is important to remember that, as shown in Eq. (5), the only manipulated variables are the blade pitch angle β and the generator torque Γ, and that at the start it was not known to the gSOC strategy if it is better to keep β constant and vary Γ, to vary β and keep constant Γ, or to vary both. As it is shown in Fig. 6(b), for region 2, the gSOC learned by itself that the optimal way to deliver the maximum power is to aim to achieve the maximum C_P, and this can be done by keeping β constant and varying Γ in such a way that the TSR is kept constant at its optimum value. If compared to the commercial wind turbine (Fig9-1 in [8]), this is the same optimum strategy, after decades of R&D and real-world experience.

Another interesting observation can be derived from Fig. 7. The fundamental difference is that, while for the BC β is kept constant at 0 deg and the TSR at values slightly lower than 7, the gSOC strategy approximate this behavior but does not replicate it exactly. The gSOC, in region 2, slightly varies both β and TSR in order to "track" the optimum C_P, since it is not constrained as the BC. Consequently, the WT controlled with the gSOC system achieves a higher coefficient of power than the BC system.

Referring to the data in Table 2, this higher efficiency does not translate into a substantially higher energy yield, since first the C_P increase is modest, and secondly in a typical turbulent wind field the wind turbine is only for a fraction of the time within the wind speed range where this advantage can be exploited.

5.2. gSOC potential

The main purpose of this work was not to augment the efficiency achieved with respect to conventional control system, but to demonstrate that a gSOC strategy can learn what is the optimum strategy without any knowledge of the model of dynamics. Furthermore, this has been achieved by using the same manipulated variables of a BC (i.e. it

can be potentially retrofitted to a commercial system) and, by considering the wind speed as a disturbance rather than as an input, in a more robust way.

The true potential can be illustrated by the question: what if the objective function J would be defined in such a way to consider also other factors? The gSOC relative simplicity, as well as its reliability, would not be compromised, since the procedure is easily scalable, and it would "suggest" what the optimum control strategy is according to this new objective. As example, it worth to recall the initial statement that modern wind turbines have access to a large amount of sensor signals, but these are used mainly to monitor the status of the wind turbine, and not to optimize the way is controlled. With the gSOC, we can for example take into account, in the objective function, the equivalent fatigue damage load at the base of the tower, or in the blades of the rotor, and make sure that the control strategy takes into account both this factor and the objective of maximizing the energy.

The long-term vision is to have a wind farm control system that has as objective function the ultimate parameter to be minimized: the Levelised Cost of Energy.

6. Conclusions and next steps

Larger and more expensive wind turbines, subject to more complex aero-hydro-servo-elastic dynamics, operating in larger wind farms (more complex turbine-to-turbine interactions), could substantially benefit from more advanced control strategies. Nonetheless, the wind industry is, in general, reluctant to adopt more advanced control strategies, and relies on simpler control structures: it is difficult to develop a control algorithm delivering both efficiency and reliability, since in general the two aspects involve conflicting objectives [1].

In the present work it has been demonstrated that a relatively simple control strategy, based on a model-free [6] global self-optimizing control methodology [7] by Cao, which already delivered promising results in the process industry, has the potential to deliver advanced control system-like performance. The gSOC strategy "re-discovered" only from operational off-line data (experience) the optimum control strategy to maximize the energy capture in region 2 adopted by the present large commercial wind turbines, i.e. "learnt to operate itself".

6.1. gSOC potential and next steps

As already proposed for other advanced control systems [1], the first step will be to include additional factors in the definition of the objective function, in order to take advantage (when defining the control strategy) of the large amount of additional sensor signals provided by the monitoring system of modern wind turbines.

The present methodology to define novel advanced control strategy offers solutions with a simplicity and reliability comparable with the simple control system adopted in the wind industry, and makes use of a simple algorithm. Nonetheless, it should not be interpreted as a substitute for the more conventional control system design techniques, relying on the definition of a model of the system. It should rather be considered as a complementary tool, which can "suggest" what could be an optimum strategy for a relatively complex dynamics system.

References

[1] J.G. Njiri, D. Soffker, State-of-the-art in wind turbine control: Trends and challenges, Renew. Sustain. Energy Rev. 60 (2016) 377–393. doi:10.1016/j.rser.2016.01.110.

[2] K.E. Johnson, Adaptative Torque Control of Variable Speed Wind Turbines, Golden, Colorado, 2004.

[3] E. Hau, H. Von Renouard, Wind turbines: fundamentals, technologies, application, economics, 2013.

[4] S. Skogestad, Plantwide control: the search for the self-optimizing control structure, J. Process Control. 10 (2000) 487–507.

[5] Y. Cao, Direct and indirect gradient control for static optimisation, Int. J. Autom. Comput. 2 (2005) 60–66.

[6] S. Adamu Girei, Y. Cao, A. Shehu Grema, L. Ye, V. Kariwala, Data-driven Self-optimizing Control, in: 2014: pp. 649–654.

[7] L. Ye, Y. Cao, Y. Li, Z. Song, Approximating Necessary Conditions of Optimality as Controlled Variables, Ind. Eng. Chem. Res. 52 (2013) 798–808

[8] J.M. Jonkman, S. Butterfield, Definition of a 5-MW reference wind turbine for offshore system development, 2009.

[9] J. Jonkman, NWTC Information Portal (FAST v8), (n.d.). https://nwtc.nrel.gov/FAST8 (accessed December 28, 2016).